Inorg. Chem. **2003**, *42*, 6780–6792

Synthesis of a Copper [3]Rotaxane Able To Function as an Electrochemically Driven Oscillatory Machine in Solution, and To Form SAMs on a Metal Surface

Noémie Weber, Christine Hamann, Jean-Marc Kern,* and Jean-Pierre Sauvage*

Laboratoire de Chimie Organo-Minérale, UMR 7513 du CNRS, Université Louis Pasteur, Faculté de Chimie, 4, rue Blaise Pascal, 67070 Strasbourg Cedex, France

Received June 20, 2003

Two new copper [3]rotaxanes have been synthesized. The axes are identical for both compounds and incorporate two bidentate chelates joined together by a disulfide bridge. The rings contain either the single phen (phen = 1,10-phenanthroline) chelate or two different chelates (phen and terpy; terpy = 2,2′,6′,2″-terpyridine, a tridentate chelate). The key intermediates for both synthetic routes are semi-rotaxanes obtained in high yields using the three-dimensional effect of copper(I). In the case where the wheels are heterobischelating macrocycles, large molecular motions, namely rotation or oscillation of the wheels around the axle, have been induced electrochemically. Anchoring of these two copper [3]rotaxanes on a gold electrode was carried out by standard procedures. Cleavage of the disulfide bridge and formation of monolayers of rotaxanes were evidenced by cyclic voltammetry. The adsorbed rotaxanes can be viewed as copper [2]rotaxanes for which the gold electrode surface acts as a stopper linked to one end of their axes.

Introduction

The field of molecular machines and motors has experienced a spectacular development in the course of the past decade.[1−3] Particularly significant are the results recently published by Stoddart, Heath, and their co-workers on molecule-based switches.[4] These devices incorporate monolayers of rotaxanes or catenanes for which the ring(s) can be shifted from a given position to another one, thus closing or opening the switch. Other spectacular examples can be found in refs 1−3, including non-catenane nor rotaxane-type organic compounds whose behavior is reminiscent of rotary motors.[3] These primitive rotary motors can be set in motion either using a photonic signal[5] or a chemical stimulus.[6]

The special feature of assemblies containing interlocked (catenanes) or threaded (rotaxanes) rings originates from the topological properties of their components: The mechanical links between the elements prevents their dissociation. As a consequence, they can undergo large amplitude but nondestructive motions in a precisely controlled fashion, and they are ideal candidates for use as molecular machines.[7,8] In this field of artificial molecular machines, our group has devoted special attention to copper-complexed catenanes and rotaxanes. Intramolecular motions of a given component of these assemblies could be triggered by varying the redox state of

* To whom correspondence should be addressed. E-mail: sauvage@chimie.u-strasbg.fr.

(1) Special issue: *Acc. Chem. Res.* **2001**, *34* (6).
(2) (a) Molecular Machines and Motors. In *Structure & Bonding*; Sauvage, J.-P., Ed.; Springer-Verlag: Berlin; 2001; Vol. 99. (b) *Molecular Switches*; Feringa, B. L., Ed.; Wiley-VCH: Weinheim, 2001.
(3) (a) Bissell, R. A.; Córdova, E.; Kaifer, A. E.; Stoddart, J. F. *Nature* **1994**, *369*, 133−137. (b) Zelikovich, L.; Libman, J.; Shanzer, A. *Nature* **1995**, *374*, 790−792. (c) Otero, T.; Sansiñena, J. M. *Adv. Mater*. **1998**, *10*, 491−494. (d) Fabbrizzi, L.; Licchelli, M.; Pallavicini, P. *Acc. Chem. Res.* **1999**, *32*, 846−853. (e) Baughman, R. H.; Cui, C.; Zakhidov, A. A.; Iqbal, Z.; Barisci, J. N.; Spinks Wallace, G. M. G. G.; Mazzoldi, A.; De Rossi, D.; Rinzler, A. G.; Jaschinski, O. S.; Roth, S.; Kertesz, M. *Science* **1999**, *284*, 1340−1344. (f) Marsella, M. J.; Reid, R. J. *Macromolecules* **1999**, *32*, 5982−5984 (g) Armarolli, N.; Balzani, V.; Collin, J.-P.; Gavina, P.; Sauvage, J.-P.; Ventura, B. *J. Am. Chem. Soc*. **1999**, *121*, 4397−4408.
(4) (a) Davis, A. P. *Nature* **1999**, *401*, 120−121. (b) Collier, C. P.; Mattersteig, G.; Wong, E. W.; Luo, Y.; Berverly, K.; Sampaio, J.; Raymo, F. M.; Stoddart, J. F.; Heath, J. R. *Science* **2000**, *289*, 1172−1175. (c) Wong, E. W.; Collier, C. P.; Béhloradsky, M.; Raymo, F. M.; Stoddart, J. F.; Heath, J. R. *J. Am. Chem. Soc.* **2000**, *122*, 5831−5840.
(5) Koumara, N.; Zijlstra, W. J.; van Delden, R. A.; Harada, N.; Ferringa, B. L. *Nature* **1999**, *401*, 152−155.
(6) (a)Kelly, T. R.; De Silva, H.; Silva, R. A. *Nature* **1999**, *401*, 150−152. (b) Kelly, T. R.; Silva, R. A.; De Silva, H.; Jasmin, S.; Zhao, Y. *J. Am. Chem. Soc.* **2000,** *122*, 6935−6949.
(7) (a) Balzani, V.; Gómez-López, M.; Stoddart, J. F. *Acc. Chem. Res.* **1998**, *31*, 405−414. (b) Balzani, V.; Credi, A.; Raymo, F. M.; Stoddart, J. F. *Angew Chem., Int. Ed.* **2000**, *39*, 3348−3391.
(8) Sauvage, J.-P. *Acc. Chem. Res.* **1998**, *31*, 611−619.

10.1021/ic0347034 CCC: $25.00
Published on Web 09/18/2003

Scheme 1. Schematic Representation of a SAM of Rotaxanes by Adsorption of a [3]Rotaxane on a Gold Surface[a]

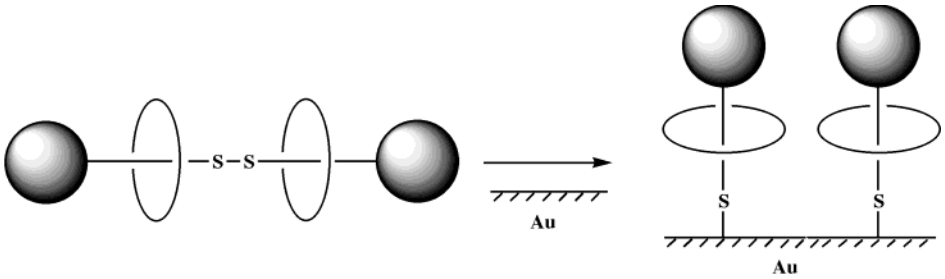

[a] In the immobilized rotaxanes, one of the end of the axis is connected to gold atoms, which acts as a blocking group, preventing dethreading of the wheel. The second blocking group (grey circle) is a purely organic bulky moiety.

the metal. Indeed, the stereoelectronic requirements of this metal depend strongly on its oxidation state: Cu(I) is normally low-coordinate whereas Cu(II) is better stabilized by penta- or hexacoordination. By reducing or oxidizing the copper center from a situation corresponding to a stable complex, the system is set out of equilibrium. The relaxation process of the compound implies a significant amplitude motion which will bring the system back to its new equilibrium position. Gliding motion of one ring around another in the case of catenanes[9] and translation[10] or oscillation[11] of a ring around a molecular thread have been studied. The assembling of switchable systems into two- or three-dimensional arrays should represent noticeable progress in the field of information storage or processing at the molecular level. Various approaches are possible. The use of switchable ionic catenanes enabled the formation of Langmuir films at an air−water interface.[12] Using a different technique, the threading or dethreading of pseudorotaxanes trapped in a rigid matrix or tethered onto a silica film could be performed.[13] One promising method for confining an active species onto a gold surface is by the formation of a Au−S bond,[14] following the strategy used successfully by several groups to make functional SAMs (self-assembled monolayers).[15] More recently, we focused our attention on monolayers of multicomponent systems organized on a metal surface. Efficient adsorption of pseudo [2]rotaxanes and [2]-catenanes was observed.[16] Through adsorption onto a gold electrode, immobilized catenanes are formed in which the gold atoms of the surface are an integral fragment of one of the rings of the catenane.

We would now like to report our efforts to make two-dimensional arrays of multicomponent molecular systems, consisting of rotaxane-like architectures anchored to a gold surface. The wheel of these rotaxanes is either a monochelating or a heterobischelating macrocycle. The axis is a coordinating molecular thread, bearing an ancillary bulky group at one end. The other end is anchored to a gold surface which plays simultaneously the role of a stopper for the rotaxane and of an input−output device between the surface-confined machine and the external source of stimuli.

These monolayers of immobilized copper [2]rotaxanes were obtained by adsorption of copper [3]rotaxanes (Scheme 1). The synthesis of two different copper [3]rotaxanes will be described as well as the "machine" behavior in solution of one of these architectures, and the first evidence of the formation of SAMs of rotaxanes onto a gold surface.

Results and Discussion

Design and Synthesis. Obviously, the shortest way to keep rotaxanes on a surface would be to adsorb a pseudo-rotaxane assembly in which the axis is linked at one end to a voluminous and chemically inert group and the other end to a thiol functionality. However, due to the pronounced reducing character of this function, the Cu center must be kept reduced (i.e., Cu(I)) until the thiolate is immobilized on the Au surface. Indeed, the corresponding copper(II) rotaxanes are strong oxidants and are not compatible with the presence of thiol functionalities.[17] In addition, ligand exchange processes around the metal can occur in the course of the adsorption process of such pseudo-rotaxanes. To overcome these difficulties, the synthesis of two different [3]rotaxanes was undertaken. The schematic and the molecular representations of these assemblies appear in Scheme 2 and in Figure 1, respectively.

The axes are identical for both rotaxanes and are composed each of two identical coordinating subunits connected to one another through a disulfide bridge. The coordinating cores are 1,10-phenanthroline moieties in which the α-positions of the nitrogen atoms are substituted with phenyl groups. Indeed, it was shown that low oxidation states of dpp-based complexes are strongly stabilized.[17,18] This is particularly true

(9) Livoreil, A.; Dietrich-Buchecker, C.; Sauvage, J.-P. *J. Am. Chem. Soc.* **1994**, *116*, 9399−9400.
(10) Collin, J.-P.; Gaviña, P.; Sauvage, J.-P. *New J. Chem.* **1997**, *21*, 525−528.
(11) Raehm, L.; Kern, J.-M.; Sauvage, J.-P. *Chem. Eur. J.* **1999**, *5*, 3310−3317.
(12) Asakawa, M.; Higuchi, M.; Mattersteig, G.; Nakamura, T.; Pease, A. R.; Raymo, F. M.; Shimizu, T.; Stoddart, J. F. *Adv. Mater.* **2000**, *12*, 1099−1102.
(13) Chia, S.; Cao, J. Stoddart, J. F.; Zink, J. I. *Angew. Chem.* **2001**, *112*, 2513−2517; *Angew. Chem., Int. Ed.* **2001**, *40*, 2447−2451.
(14) (a) Lu, T.; Zhang, L.; Gokel, G. W.; Kaifer, A. E. *J. Am. Chem. Soc.* **1993**, *115*, 2542−2543. (b) Rojas, M. T.; Kaifer, A. E. *J. Am. Chem. Soc.* **1995**, *117*, 5883−5884.
(15) Ulman, A. *Chem. Rev.* **1996**, *96*, 1533−1554 and references therein.
(16) (a) Kern, J.-M.; Raehm, L.; Sauvage, J.-P. *C. R. Acad. Sci., Ser. IIc: Chim.* **1999**, 41−47. (b) Raehm, L.; Hamann, C.; Kern, J.-M.; Sauvage, J.-P. *Org. Lett.* **2000**, *14*, 1991−1994. (c) Raehm, L.; Kern, J.-M.; Sauvage, J.-P.; Hamann, C.; Palacin, S.; Bourgoin, J.-P. *Chem. Eur. J.* **2002**, *8*, 2153-2162.
(17) The redox potential of CuII/I bis(2,9-diaryl)1,10-phenanthrolines is located around 0.6 V vs SCE: (a) Federlin, P.; Kern, J.-M.; Rastegar, A.; Dietrich-Buchecker, C.; Marnot, P. A.; Sauvage, J.-P. *New J. Chem.* **1990**, *14*, 9−12. (b) Balzani, V. In *Electron Transfer in Chemistry*; Balzani, V., Ed.; Wiley-VCH: Weinheim, 2001; Vol 3, p 582−650.

Scheme 2. Schematic Representation of Copper [3]Rotaxanes **A** and **B**[a]

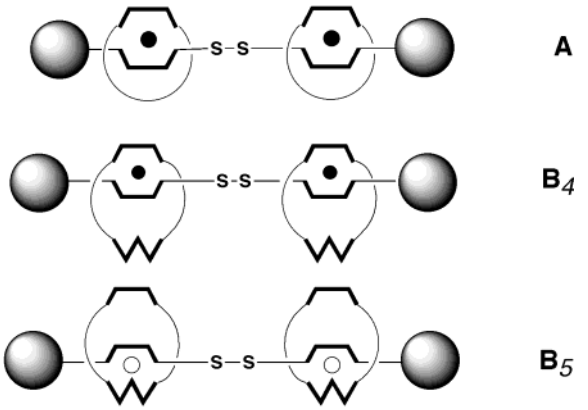

[a] The axes of **A** and **B** are identical. They incorporate two bidentate ligands, each. In **A**, the wheels are monochelating macrocycles, each. In **B**, the wheels of the rotaxane incorporate a bidentate and a terdentate site, each. Consequently, the metal centers can be either tetracoordinated, situation $\mathbf{B}_4$, or pentacoordinated, situation $\mathbf{B}_5$. The black circle represents Cu(I), and the white circle represents Cu(II).

for copper complexes. A hexamethylene chain joins together the coordinating 2,9-bis(*p*-phenoxy)-1,10-phenanthroline moieties and the disulfide bridge. The two end groups of the thread, that is, the stoppers of the [3]rotaxanes, are tetraarylmethane derivatives. In order to increase the size of the stoppers and to lower solubility problems, lipophilic groups (*tert*-butyl fragments) were introduced on the para positions of three of the aryl groups. The stoppers and the coordinating sites are linked through bis-ethoxy-ether spacers. Two monochelating or two bisheterochelating macrocycles form the wheels of [3]rotaxanes **A** and **B** (Scheme 2), respectively. The monochelating ring (Figure 1) contains one coordinating site, a dpp (dpp = 2,9-diphenyl-1,10-phenanthroline), whose end positions are connected through a pentaethyleneglycol chain. The bis-heterochelating ring (Figure 1) contains two different coordinating sites: a terpyridine moiety and a dpp one. The two units are joined through two C_3 chains which are linked to the 5,5″-positions of the terpyridine on one side and to the oxygen atoms of the 2,9-bis(4-oxyphenyl)-1,10-phenanthroline on the other side. In both [3]rotaxanes, the axle and the wheels are connected together through the coordinated copper ions. More precisely, in [3]rotaxane **A** (Scheme 2), the metal centers, whatever their oxidation state, are tetracoordinated, the thread and the wheels providing each a bidentate site to each metal. The situation is different for [3]rotaxane **B** (Scheme 2): the wheels provide a bidentate or a terdentate site each, and consequently, the coordination number *N* of the metal centers is either 4 or 5. Cu(I) is most of the time low-coordinate ($N \leq 4$) whereas Cu(II) is preferably square planar or higher coordinate ($N = 5$ or 6). Scheme 2 represents rotaxane **B** in these two different situations: $\mathbf{B}_5$ corresponds to the situation in which the two metal centers (Cu(II)) are pentacoordinated, and $\mathbf{B}_4$ corresponds to the situation in which the metals (Cu(I)) are tetracoordinated. Thus, varying the oxidation state of the metal can lead to a large rearrangement of the surrounding ligands. By using this phenomenon, the gliding of a ring within another one in the case of catenanes, the translation of a ring along a molecular thread or the oscillation of a ring around a thread in the case of rotaxanes, could be triggered and monitored.[9−11] Presently, we would like to describe the synthesis, the electrochemical behavior of these [3]rotaxanes in solution, and the first results on our attempts to prepare rotaxane-like monolayers at a gold surface.

The main sequences leading to the two copper [3]rotaxanes described here are represented in Scheme 3. A molecular thread was prepared at first (Scheme 3a) which consists of a dpp-type ligand connected to a bulky ancillary group at one extremity and to a stable thiol precursor functionality at the other one. During the second step (Scheme 3b,c), two different semi-rotaxanes are formed by threading this segment through either a mono- or a bischelating macrocycle.

Scheme 3. Principle of the Synthesis of Rotaxanes **A** ($Cu_2\mathbf{12}^{2+}$) and **B** ($Cu_2\mathbf{15}^{2+}$)[a]

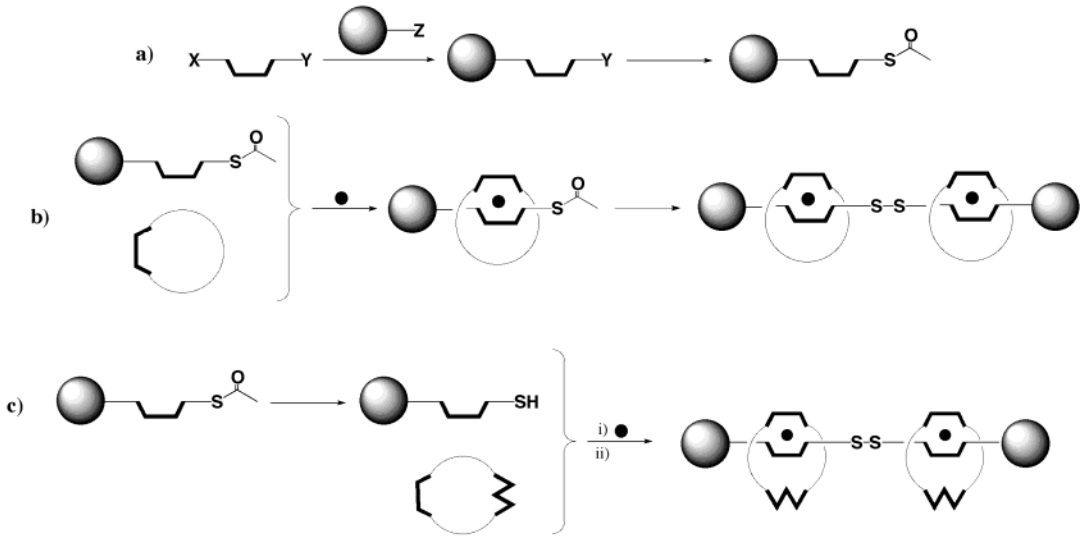

[a] Steps of the syntheses are the following: (a) formation of a monostoppered axis, bearing a precursor of a thiol functionality at one end, (b) threading of the axis through the wheel, hydrolysis of the thioacetate, and oxidative dimerization [this strategy was used to synthesize **A** ($Cu_2\mathbf{12}^{2+}$)], or (c) hydrolysis of the thioacetate group occurred, threading of the resulting axis through the wheel (i) followed by oxidative dimerization (ii). This strategy was used to synthesize $\mathbf{B}_4$ ($Cu_2\mathbf{15}^{2+}$). The black circle represents Cu(I); the large gray circle represents the blocking group linked to the end of the axis.

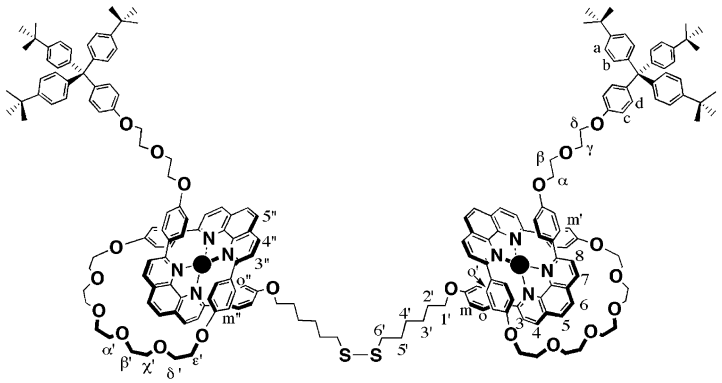

Cu_2**12**$^{2+}$

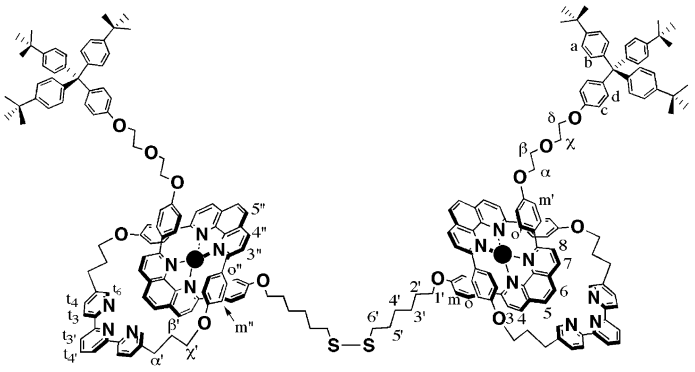

Cu_2**15**$^{2+}$

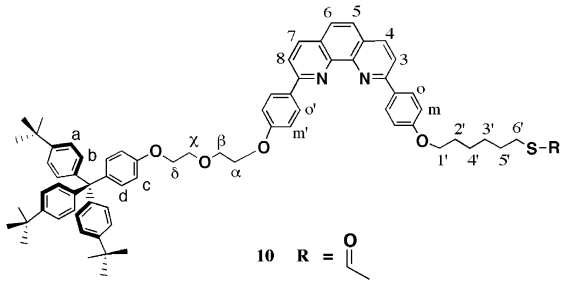

10 R =

13 R = H

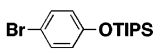

1

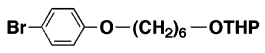

3

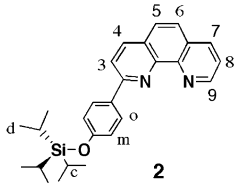

2

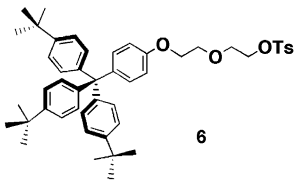

6

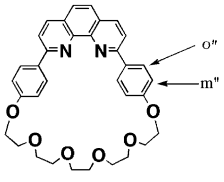

11

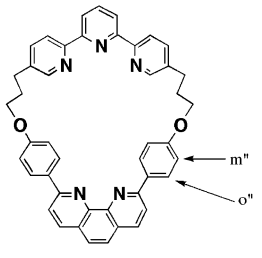

14

Figure 1. Representation of the copper-complexed [3]rotaxanes Cu_2**12**$^{2+}$ and Cu_2**15**$^{2+}$, and of their precursors. **13** is the precursor of the axis of both rotaxanes. Macrocycles **11** and **14** are the wheels of rotaxanes Cu_2**12**$^{2+}$ and Cu_2**15**$^{2+}$, respectively. Ring **11** includes a dpp unit as coordinating site. Ring **14** includes both a bidentate (dpp) and a tridentate (terpy) coordinating site.

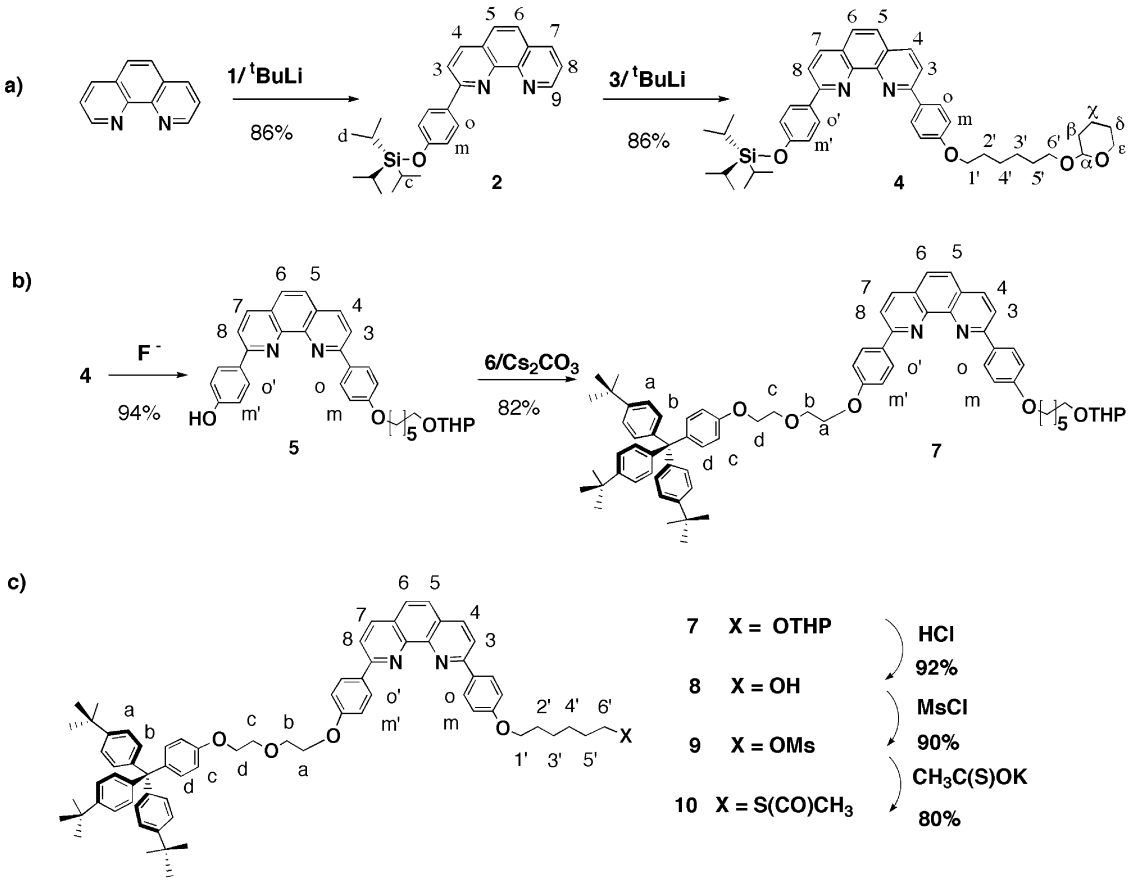

Figure 2. Synthetic route leading from 1,10-phenanthroline to the molecular thread **10**. (a) Disymmetrization of the phenanthroline by substituting positions 2 and 9 with two different protected functionalities. (b) Desilylation of the phenoxy functionality and subsequent grafting of the bulky tetraaryl methane derivative. (c) Introduction of a thiol precursor at the end position of the thread.

These threading operations were done before (Scheme 3b) or after (Scheme 3c) hydrolysis of the thiol precursor. Finally, clipping of each semi-rotaxane with itself by using a mild oxidative reagent led to the two expected [3]rotaxanes.[19] Their molecular representation, as well as that of the various synthetic intermediates, is given in Figure 1. The synthetic route leading to the functionalized monostoppered segment is described in Figure 2.

Heterobifunctionalization of 1,10-phenanthroline (Scheme 3a and Figure 2a) was made in two steps: the controlled addition of the lithio-derivative of silylated *p*-bromophenol **1** on 1,10-phenanthroline led, after hydrolysis and oxidation of the adduct, to the monosubstituted phenanthroline **2**. Addition in a similar manner of the lithio derivative of **3** on **2** led to the 2,9-diaryl-phenanthroline **4** in which the two para positions of the phenyl groups bear two different, protected, functionalities. The overall yield, based on 1,10-phenanthroline, is 74%. By desilylating **4** and reacting the resulting phenol **5** with the stopper **6**, one could obtain the monostoppered thread **7** in an overall yield of 77%, based on **4** (Figure 2b). Figure 2c represents the three-step sequence which leads from **7** to compound **10**, in which the air stable $SCOCH_3$ functionality is linked to the coordinating moiety via a hexamethylene spacer. This was done by hydrolysis of the tetrahydropyranyl ether **7**, esterification of the resulting alcohol **8** into **9**, which was subsequently transformed into **10** by treatment with potassium thioacetate. At this stage, the routes leading to the two [3]rotaxanes became different (Scheme 3 and Figure 3). Semi-rotaxane Cu(**10**.**11**)$^+$ was prepared in the following manner (**11** is a 30-membered monochelating macrocycle, represented Figure 1): $Cu(CH_3CN)_4BF_4$ was added to a solution of **11** in CH_2Cl_2/CH_3CN. The resulting orange solution was then treated with **10** to give a dark-red solution of hemi-rotaxane Cu(**10**.**11**)$^+$. The almost quantitative yield of this threading reaction originates from the exceptional stability of Cu(I)−bis(dpp)-derivative complexes.[20] Semi-rotaxane Cu(**10**.**11**)$^+$ was refluxed in air with a catalytic amount of HBF_4. Copper(I) [3]rotaxane Cu_2**12**$(BF_4)_2$ was isolated in 50% yield after purification by chromatography. ^{1}H NMR spectra of Cu_2(**12**)$^{2+}$ and semi-rotaxane Cu(**10**.**11**)$^+$ are quite similar, with a noticeable exception for the signals H6′ in α position of the sulfur atoms, for which a shielding of $\Delta\delta = 0.13$ ppm is observed when going from the H6′ protons in Cu(**10**.**11**)$^+$ to the corresponding protons in Cu_2**12**$^{2+}$. Entwining of the dpp moieties around the metal center was clearly observed by

(18) Dietrich-Buchecker, C.; Kern, J.-M.; Sauvage, J.-P. *J. Am. Chem. Soc.* **1989**, *111*, 7791−7800.

(19) An analogous molecular *riveting* reaction was described recently by Bush and al.: Kolchinski, A. G.; Alcock, N. W.; Roesner, R. A.; Bush, D. H. *Chem. Commun.* **1998**, 1437−1438.

(20) Arnaud-Neu, F.; Marques, E.; Schwing-Weill, M.-J.; Dietrich-Buchecker, C. O.; Sauvage, J.-P.; Weiss, J. *New J. Chem.* **1988**, *12*, 15−20.

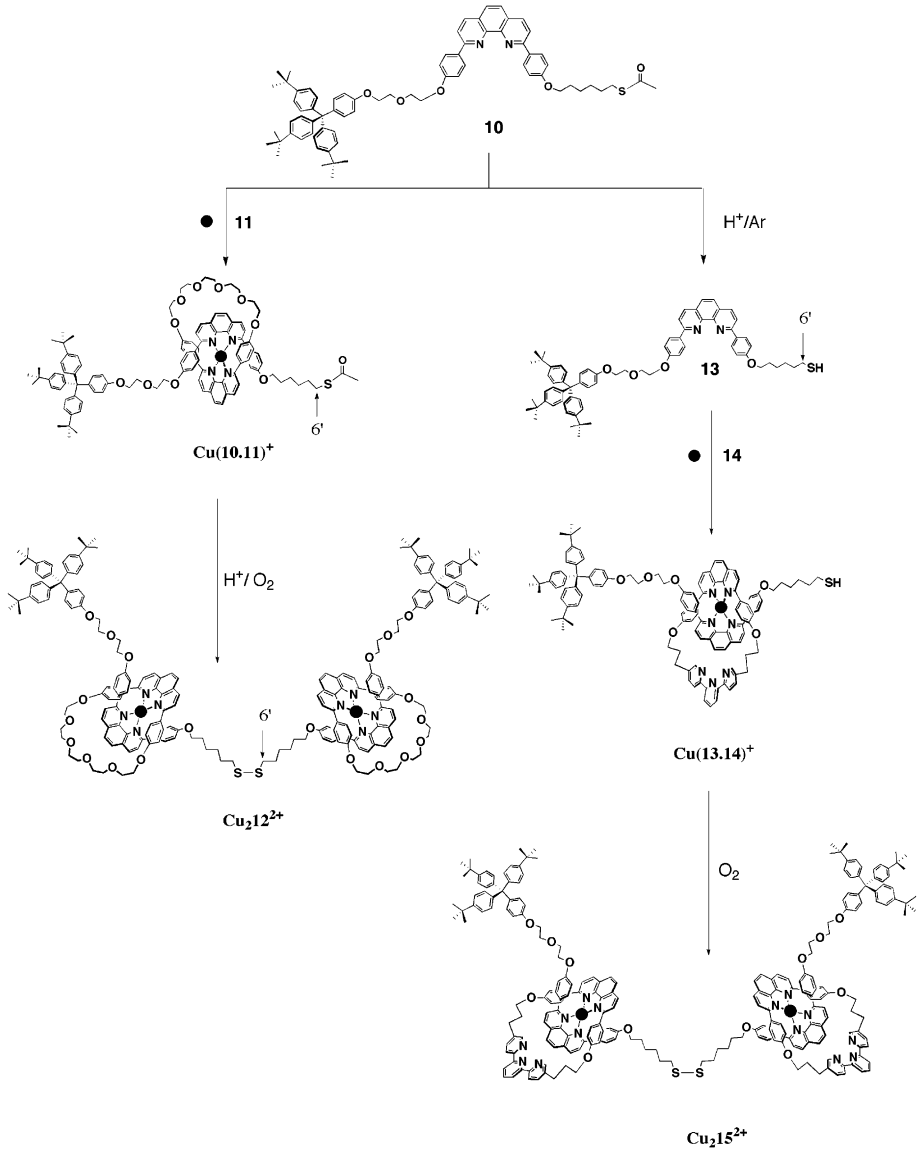

Figure 3. Representation of the threading and riveting reactions which are the key steps of the synthesis of [3]rotaxanes Cu_2**12**$^{2+}$ and Cu_2**15**$^{2+}$. Cu_2**12**$^{2+}$: ring **11** is threaded on the linear fragment **10** before the hydrolysis of the thioacetate functionality and riveting of the resulting semi-rotaxane Cu(**10.11**)$^+$. Cu_2**15**$^{2+}$: The hydrolysis of the linear fragment **10** is performed before its threading through ring **14**. Riveting of the resulting semi-rotaxane Cu(**13.14**)$^+$ is done by stirring a dichloromethane solution of Cu(**13.14**)$^+$ in air. The black circle represents Cu(I).

^{1}H NMR. The meta protons Hm, Hm′, and Hm″ (Figure 1) of the three nonequivalent phenoxy moieties in Cu_2**12**$^{2+}$ resonate at a significantly higher field than the corresponding protons in the free macrocycle **11** and in **7** (Figure 4). For instance, a shielding of $\Delta\delta = 0.11$ ppm is observed from the meta protons Hm" of the free ring **11** to the corresponding protons in Cu**12**$^{2+}$. In the thread **10**, the external (Hm′) and internal (Hm) meta protons are nonequivalent. A similar shift, $\Delta\delta = 1.04$ ppm, is observed for these protons after threading of **10** through macrocycle **11**, i.e., when going from **10** to Cu(**10.11**)$^+$ and to Cu_2**12**$^{2+}$. The ratio of the relative intensities of the signals corresponding to the meta protons of the linear fragment, i.e., Hm and Hm′, to the meta protons Hm″ of the macrocycle is in accordance with the expected value.

FAB-MS spectroscopy confirmed the structure of Cu_2**12**$^{2+}$-$(BF_4^-)_2$. Intense peaks (Figure 5) are observed at m/z = 3455.9 (M − BF_4)$^+$, 3369.2 (M − 2BF_4 + 1e)$^+$, 2738.5 (M − **11** − Cu − 2BF_4)$^+$, 1684.0 (M − 2BF_4)$^{2+}$/2, 629.3 (**11** + Cu)$^+$. Noteworthy are the peaks at m/z = 2738.5 and 2172.2 corresponding to the loss of one and of both threaded macrocycles **11**, respectively.

The route leading to [3]rotaxane Cu_2**15**$^{2+}$ is slightly different from that leading to Cu_2**12**$^{2+}$. Threading of the heterobischelating macrocycle **14** onto **10** occurred as efficiently as for macrocycle **11**, but hydrolysis of the resulting semi-rotaxane Cu(**10.14**)$^+$ is accompanied by the dethreading of the ring. To overcome this difficulty, the free compound **10** was hydrolyzed in a strictly oxygen free atmosphere. The resulting thiol-functionalized linear fragment **13** was not further stored but was immediately threaded through macrocycle **14**, following the same procedure as described. The resulting semi-rotaxane Cu(**13.14**)$^+$, in solution in CH_3CN/CH_2Cl_2, was stirred for 2 h in air. Treatment of the crude reaction product allowed us to isolate pure copper [3]rotaxane Cu_2**15**$(BF_4)_2$ in 52% yield. ^{1}H NMR and

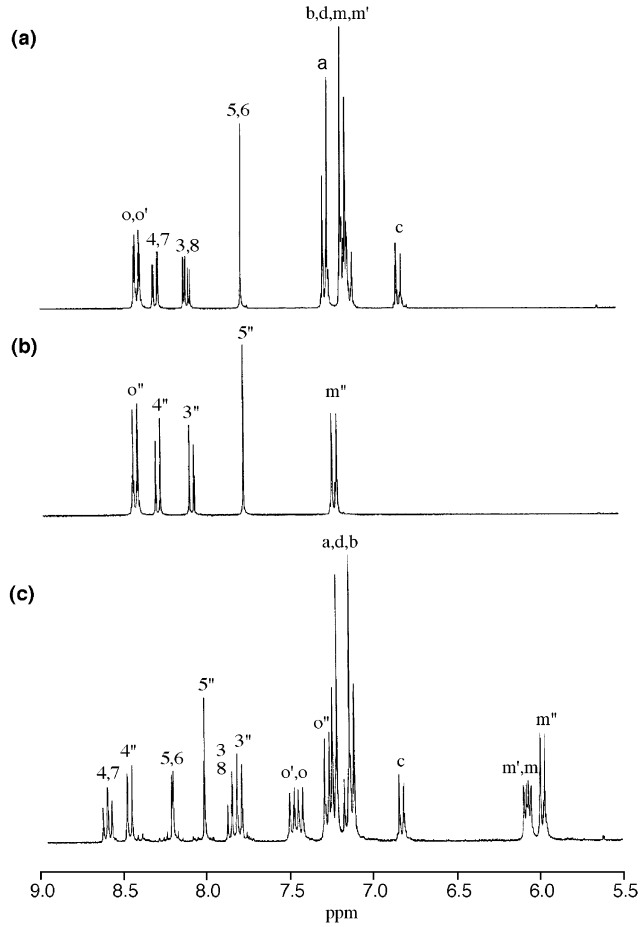

Figure 4. Upfield shifts of the protons ortho and meta of the different dpp units in [3]rotaxane Cu_2**12**$^{2+}$: representation of the ^{1}HNM spectra of thread **10** (spectrum a), macrocycle **11** (spectrum b), and copper-complexed [3]rotaxane Cu_2**12**$^{2+}$. Peaks labeled o, m and o′, m′ refer to ortho and meta protons of, respectively, the internal and external phenyl groups of the thread (labeling of the protons appears in Figures 1−3). Peaks labeled o″ and m″ refer respectively to ortho and meta protons of the ring. The nonequivalence of protons m, m′, and m″ as well as that of protons o, o′, and o″ appears distinctly on spectrum c.

FAB-MS spectra are analogous to those of Cu_2**12**$^{2+}$ and in full accordance with the expected structure of Cu_2**15**$^{2+}$. Moreover, ^{1}H NMR spectroscopy shows clearly that the dpp moieties of the rings **14** are entwined around the metal centers. As macrocycle **14** allows the metal to be either tetra- or pentacoordinate, this observation underlines the preference of Cu^I for tetracoordination.

Electrochemical Behavior of the Copper-Complexed [3]-Rotaxanes $Cu_2$12^{2+} and $Cu_2$15^{2+}. Observation of the Spinning of the Wheels around the Axle in [3]Rotaxane $Cu_2$15^{2+}. The thermodynamics of Cu(dpp-based)$_2$ and Cu(dpp−terpy-based) complexes is well-known.[17] The $Cu^{II/I}$ redox potential is relatively high for the former (0.6−0.7 V vs SCE), that is, for tetracoordinated copper, and markedly more cathodic for the second family of complexes (0 to −0.5 V vs SCE), that is, for pentacoordinated copper. The behavior of Cu_2**12**$^{2+}$ is characteristic of assemblies incorporating Cu(dpp)$_2$ moieties: in CH_2Cl_2/CH_3CN, a reversible signal is observed at 0.68 V versus SCE, and no electronic coupling between the two redox centers can be detected (Figure 1 in Supporting Information). [3]Rotaxane Cu_2**15**$^{2+}$ displays a similar behavior (Figure 6a represents the anodic scan of the CV, and Figure 2a in Supporting Information is the complete CV): the two metal centers are tetracoordinated, and their redox potential is localized at 0.62 V versus SCE (ΔE_p = 80 mV). The ratio of the intensities of the anodic and cathodic peaks is close to 1 and shows that no transformation or reorganization of the coordination sphere of the tetracoordinate Cu(II) centers occurs in the time scale of the measurements (potential sweep rate: 100 mV s^{-1}) despite the presence of the terpy moiety in the wheels of the rotaxane. But by changing drastically the time scale of the experiment, substitution of the dpp sites of the wheels by the terpy-sites in the copper(II) [3]rotaxane occurred. This was performed by doing an exhaustive anodic oxidation of Cu_2**15**$^{2+}$ in CH_2Cl_2/CH_3CN at a platinum electrode polarized at 0.8 V versus SCE. The red color of the copper(I) rotaxane disappeared, and the solution became green. The cyclic voltammetry behavior of the resulting Cu(II) rotaxane Cu_2**15**$^{4+}$ is totally different from that of Cu_2**12**$^{2+}$. The potential sweep for the measurement was started at +0.9 V, a potential at which no electron transfer should occur, regardless of the nature of the surrounding of the Cu(II) center (penta- or tetracoordination). An irreversible peak is observed at −0.1 V and is assigned to the reduction of the pentacoordinated complex (Figure 6b represents the cathodic scan of the CV, and Figure 2b in Supporting Information is the complete CV). The irreversibility of this peak means that the pentacoordinated Cu(I) species formed in the diffusion layer, when sweeping cathodically the electrode potential, is transformed very rapidly into a new species, electrochemically silent in this cathodic potential range. Moreover, the appearance of an anodic peak at 0.64 V suggests that the transient species formed by reduction of Cu_2**15**$^{4+}$ has undergone a complete reorganization which leads to a tetracoordinated copper(I) rotaxane.

This cyclic voltammetric experiment done after exhaustive anodic oxidation of Cu_2**15**$^{2+}$ shows that in the time scale of the electrolysis (around 15 min) the rotation of the two wheels around the axle is complete. These motions allow the relaxation of the electrogenerated Cu(II)-complexed [3]-rotaxane, by leading from a situation in which Cu(II) is only tetracoordinated to a more stable situation in which each Cu(II) is coordinated to five nitrogen atoms. Conversely, the irreversibility (at 100 mV s^{-1}) of the reduction peak of Cu_2**15**$^{4+}$, where the two metal centers are pentacoordinated, shows that here again, although very rapidly, the system relaxes by a new rotation of the rings to offer a tetracoordination to the Cu(II) centers. Moreover, by changing the time scale of the CV experiments, i.e. by increasing the potential sweep rate, the system becomes progressively reversible, as expected for the case where an electron transfer is followed by an irreversible chemical reaction. This was confirmed by the data analysis of the *I*/*E* (current/potential) responses, following the method described by Nicholson and Shain,[21] and already used for the determination of the spinning motion of a ring around an axle in a [2]rotaxane.

(21) Nicholson, R. S.; Shain, I. *Anal. Chem.* **1964**, *36*, 706−723.

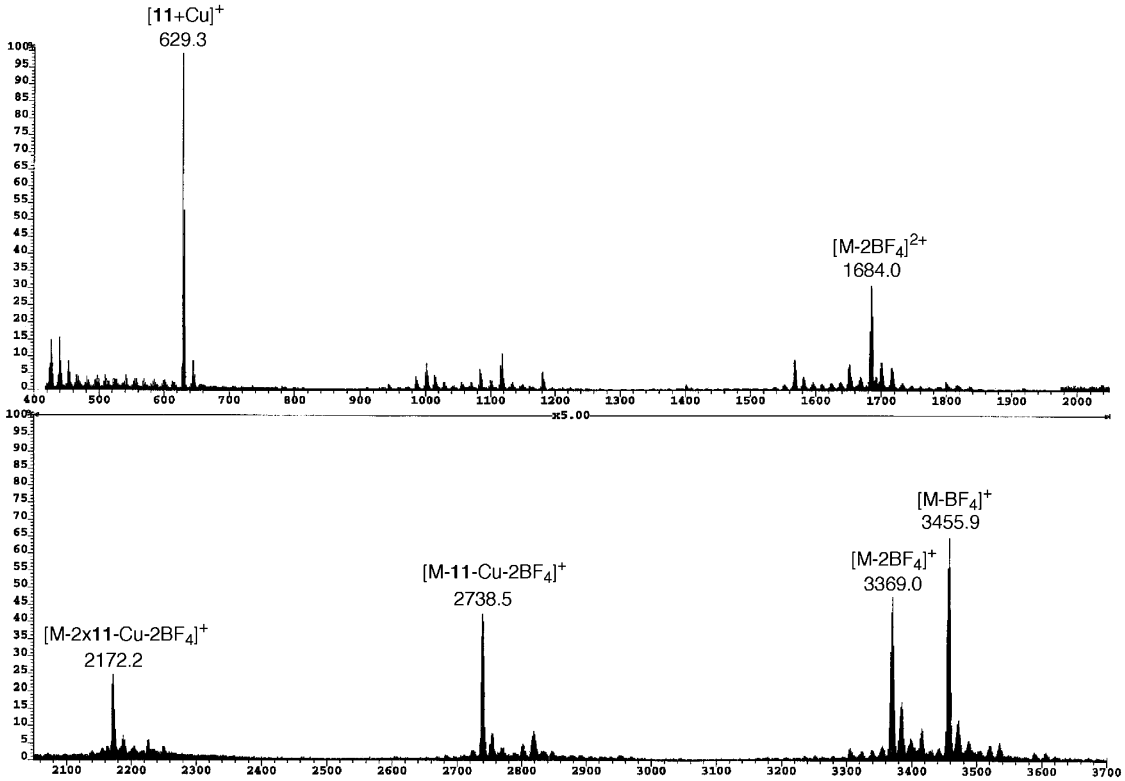

Figure 5. FAB-MS spectrum of [3]rotaxane $Cu_2\mathbf{12}^{2+}$. The stepwise fragmentation and subsequently loss of the two wheels is obvious and characterized by the peaks ($[M - \mathbf{11} - Cu - 2BF_4]^+$, $m/z = 2738.5$) and ($[M - 2(\mathbf{11}) - Cu - 2BF_4]^+$, $m/z = 2172.2$). Fragmentation of the axis leads to $[\mathbf{11} + Cu]^+$, ($m/z = 629.3$).

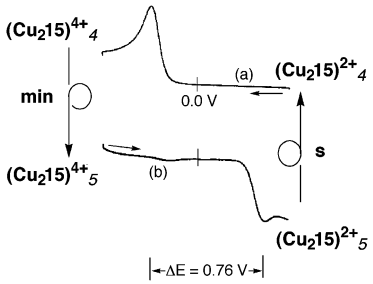

Figure 6. Voltammetry curves recorded using a Pt working electrode at a 100 mV s^{-1} potential sweep rate (CH_3CN/CH_2Cl_2 (4:1), Bu_4NBF_4 0.1 mol L^{-1}). A $Hg/HgSO_4$ electrode was used as reference electrode. (a) Cu(I)-complexed [3]rotaxane $Cu_2\mathbf{15}^{2+}$. Anodic potential sweep. The metal centers are tetracoordinated. (b) Cu(II)-complexed [3]rotaxane $Cu_2\mathbf{15}^{4+}$. Cathodic potential sweep. $Cu_2\mathbf{15}^{2+}$ was obtained by anodic oxidation of $Cu_2\mathbf{15}^{2+}$. The voltammogramm was recorded immediately after the electrolysis. The cathodic peak at −0.41 V corresponds to the reduction of the pentacoordinated metal centers.

An average value of 1.0 ± 0.3 s^{-1} was found for the spinning rate constant *k*. Thus, in the experimental conditions, i.e., acetonitrile/dichloromethane (4/1), Bu_4NBF_4 10^{-1} mol L^{-1}, the half-life time of the bis-pentacoordinated bis-Cu^I [3]-rotaxane is 700 ± 200 ms. The overall process is represented in Figure 6. In the system described in this work, the reorganization rates of the ligand set around the metal centers remain high by comparison with those observed in a catenane[9] or in a rotaxane where the axle is a hetero-bischelating molecular thread and the wheel a monochelating macrocycle.[10] Nevertheless, comparison with the structurally analogous copper complexed [2]rotaxane synthesized and studied in previous work[11] shows that the spinning rates around pentacoordinated Cu(I) significantly decrease when going from the [2]rotaxane[11] to the [3]rotaxane, $Cu_2\mathbf{15}^{2+}$. Indeed, a half-life time value of 0.056 s was determined for the pentacoordinated copper(I) in the [2]rotaxane,[11] the corresponding values for the [3]rotaxane $(Cu_2\mathbf{15}^{2+})_5$ being 0.7 s (*4* and *5* refer to the coordination number of the metal). The spinning rate around tetracoordinated Cu(II) in $(Cu_2\mathbf{15}^{4+})_4$ has the same order of magnitude as that observed for the [2]rotaxane,[11] i.e., a half-life time $t_{1/2}$ of minutes. Unfortunately, due to adsorption of the substrate on the working electrode, a more accurate value for $t_{1/2}$ of $(Cu_2\mathbf{15}^{4+})_4$ could not be obtained.

Monolayers of Rotaxanes. Deposition onto a Gold Surface. In the preliminary attempts described here to prepare surface confined rotaxanes, $Cu_2\mathbf{12}^{2+}$ and $Cu_2\mathbf{15}^{2+}$ were deposited onto gold surfaces, and the adsorption processes were followed by cyclic voltammetry. Gold bead electrodes were dipped over 2 and 5 h into dichloromethane solutions of $Cu_2\mathbf{12}^{2+}$ and $Cu_2\mathbf{15}^{2+}$, respectively. After the adsorption time, the gold beads were thoroughly rinsed with dichloromethane, dipped into dichloromethane containing only Bu_4NBF_4 as supporting electrolyte, and used as working electrodes. Figure 7 depicts the characteristic curves, recorded at different potential sweep rates, after dipping gold bead electrodes in solutions of $Cu_2\mathbf{12}^{2+}$ (Figure 7a) and $Cu_2\mathbf{15}^{2+}$ (Figure 7b). The presence of a reversible electron transfer in each case is obvious, and the half-wave potential values ($E_{1/2} = 0.56$ V for $Cu_2\mathbf{12}^{2+}$, $E_{1/2} = 0.58$ V for $Cu_2\mathbf{15}^{2+}$) attest to the presence on the working electrodes of the Cu−bisdiaryl phenanthroline moieties in each case. The ΔE_p values (ΔE_p is the difference in potential between the oxidation and

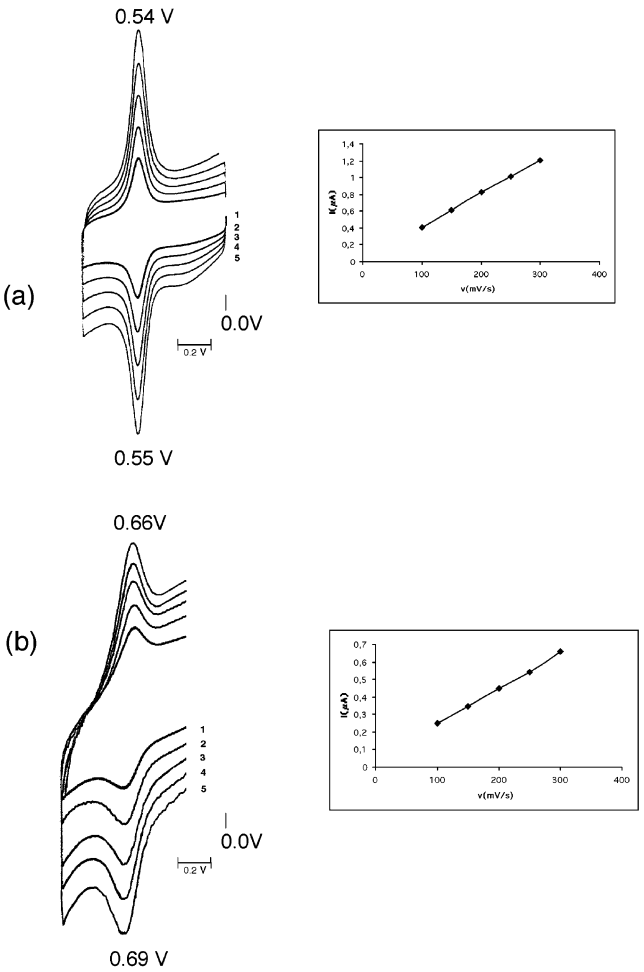

Figure 7. Cyclic voltammetry responses of a gold bead electrode (CH_2Cl_2, 10^{-1} mol L^{-1} Bu_4NBF_4) after being dipped in CH_2Cl_2 solutions (10^{-3} mol L^{-1}) of rotaxanes Cu_2**12**$^{2+}$ (a) and Cu_2**15**$^{2+}$ (b) and rinsed. Potential sweep rates: (1) 50 mV s^{-1}, (2) 100 mV s^{-1}, (3) 200 mV s^{-1}, (4) 200 mV s^{-1}, and (5) 400 mV s^{-1}. Increasing of the oxidation current peak with the potential sweep rate is represented in the two inserts in parts a and b.

reduction peaks) are less than 60 mV for each adsorbed species (20 mV for Cu_2**12**$^{2+}$ and 30 mV for Cu_2**15**$^{2+}$ at 100 mV s^{-1} in each case). The intensity of the anodic and cathodic peaks increases linearly with the potential sweep rate, for both adsorbed species as represented in the inserts of Figure 7. All these observations are in accordance with the presence of immobilized electroactive species at the gold surface.

The adsorbed layers resist several redox scans (after 60 scans, a decrease of only 20% of the electroactivity of adsorbed Cu_2**15**$^{2+}$ observed, for example). This stability is consistent with an Au−S bond formation along with the adsorption process. The disulfide bridges in Cu_2**12**$^{2+}$ and in Cu_2**15**$^{2+}$ are likely to be cleaved[14b,15] leading to two Au−S bonds in each case. Consequently, one can assume that the copper [3]rotaxanes Cu_2**12**$^{2+}$ and Cu_2**15**$^{2+}$ are converted, respectively, to copper [2]rotaxanes Cu**16**$^{+}$(ads) and (Cu**17**$^{+}$)$_4$(ads), one stopper remaining a tetraaryl moiety, and the gold atoms of the adsorbate's host forming the second stopper (Scheme 1 and Figure 8):

$$Cu_2\mathbf{12}^{2+} + Au \rightarrow 2Cu\mathbf{16}^{+}(ads)$$

and

$$Cu_2\mathbf{15}^{2+} + Au \rightarrow 2(Cu\mathbf{17}^{+})_4(ads)$$

The molecular-machine-like behavior of [3]rotaxane Cu_2**15**$^{2+}$ was discussed in the previous section. The fast gliding of the rings around pentacoordinated Cu^{I} and the significantly slower motion around tetracoordinated Cu^{II} were demonstrated. The CV curves represented in Figure 7b show that, when going from the rotaxane in solution to the surface confined species, the oxidation process, i.e, (Cu**17**$^{+}$)$_4$(ads) → (Cu**17**$^{2+}$)$_4$(ads), remains reversible. Any modification of the cathodic branch of the CV curve was observed even when the electrode potential was polarized at a positive value (0.8 V) for a certain period of time, and no well-defined reduction peak localized around −0.1 V appeared. This seems to indicate that, as for the molecular [3]rotaxane in solution, the spinning of the wheel around Cu^{II} is too slow to be detected on the time scale of the CV measurement. Conversely, adsorption onto gold of (Cu_2**15**$)^{4+}{}_5$ whose metal centers are pentacoordinated (vide supra) led only to unstable adsorbates, whose responses to electrochemical inputs are not reproducible. It is noteworthy that the same difficulty was encountered in previous works in efforts to anchor Cu^{II} catenanes on gold. Work is in progress to understand this phenomenon and to overcome these difficulties.

Conclusion

The synthesis of two copper [3]rotaxanes is described. In each case, the axle of the assembly includes two 2,9-diaryl-1,10-phenanthroline sites connected together by a disulfide bridge. The wheels of these rotaxanes are either two identical monochelating macrocycles or two identical heterobischelating macrocycles. The synthetic routes are very similar. The two key steps are the formation of a semi-rotaxane, based on the template effect of Cu^{I}, followed by its oxidative coupling. A molecular machine behavior was observed in solution for the [3]rotaxane in which the wheels incorporate a terdentate site as well as a bidentate one. By varying the redox state of the coordinated metal centers, reversible spinning of the rings around the axis could be observed, although the spin rates around Cu^{I} and Cu^{II} are markedly different. Adsorption experiments demonstrated the possibility of preparing layers of electroactive rotaxanes onto a gold surface. The metal electrode acts simultaneously as a stopper and as an input−output gate for the redox processes. Combined STM−electrochemical studies are in progress in order to trigger and subsequently to visualize rotation of the ring around the axis in surface confined molecular machines.

Experimental Section

General Methods. Oxygen- or water-sensitive reactions were conducted under a positive pressure of argon in oven-dried glassware, using Schlenk techniques. Column chromatography was carried out on silica gel 60 (E. Merck, 70−230 mesh) or on aluminum oxide 90 standardized (E. Merck). ^{1}H NMR spectra were obtained on either a Brucker WP 200 SY (200 MHz) or an AM

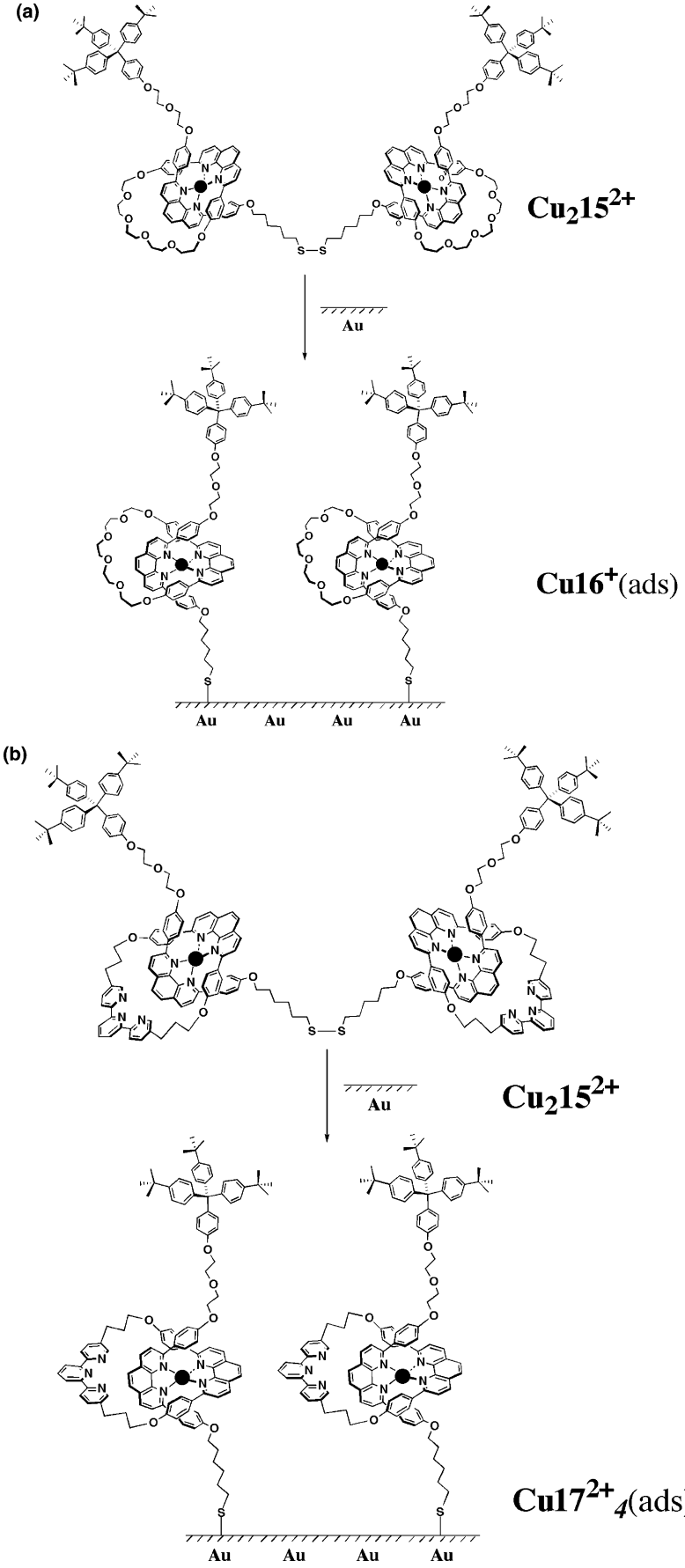

Figure 8. Schematic representation of the adsorption process leading from the true copper-complexed [3]rotaxanes Cu_2**12**$^{2+}$ (a) and Cu_2**15**$^{2+}$ (b) in solution to the surface confined [2]rotaxanes Cu**16**$^{+}$(ads) and Cu**17**$^{+}{}_4$(ads), respectively. The gold atoms of the host metal act as a stopper for the immobilized copper-complexed [2]rotaxanes.

400 (400 MHz) spectrometer. NMR chemical shifts δ are expressed in ppm relative to internal solvent peaks. Labels of the protons of semi-rotaxane Cu(**10.11**)$^+$ and Cu(**13.14**)$^+$, of [3]rotaxanes Cu_2**12**$^{2+}$ and Cu_2**15**$^{2+}$, and of their precursors are provided in Figures 1−3. Fast atom bombardment mass spectrometry (FAB MS) data were recorded in the positive ion mode with a xenon primary atom beam in conjunction with a 3-nitrobenzyl alcohol matrix and a ZAB-HF mass spectrometer. A VG BIOQ triple quadrupole spectrometer was used for the electrospray mass spectrometry measurements (ES-MS) also in the positive ion mode. Electrochemical experiments were carried out using a EGG Princeton 273 A model potentiostat equipped with an X-Y recorder (Research Electrochemistry Software). All experiments were run at room temperature. A standard three-electrode cell was used. For the measurements performed on the rotaxanes in solution, the potentials were determined either with a mercury sulfate reference electrode or with a Ag wire pseudo-reference electrode and referenced to SCE using ferrocene as internal reference. For the measurements performed on the gold adsorbates, the potentials are only referenced to the Ag wire pseudoreference electrode. Tetrabutylammonium tetrafluoroborate (0.1 mol L^{-1}) in an acetonitrile/dichloromethane 4/1 mixture was used as supporting electrolyte. A platinum disk electrode (2 mm diameter) was used for CV experiments of the [3]rotaxanes in solution. The gold bead working electrodes were made by annealing the tip of a gold wire (99.9985%, 0.5 mm diameter) in a gas−oxygen flame. After being cooled, the gold bead was immersed in a $\sim 10^{-3}$ mol L^{-1} solution of the [3]rotaxanes Cu_2**12**$^{2+}$ or Cu_2**15**$^{2+}$ in CH_2Cl_2 for times varying from 10 min to 18 h. The electrode was then washed with pure CH_2Cl_2. A platinum wire (0.6 mm diameter, 52 cm long) was used as working electrode for electrolysis at controlled potential.

Synthesis. Common reagents and materials were purchased from commercial sources. The following materials were prepared according to literature procedures: **1**,[22] **6**,[23] **11**,[24] **14**,[25] $Cu(CH_3CN)_4BF_4$.[18]

Monofunctionalized Phenanthroline 2. Compound **1** (5.49 g, 16.7 mmol) was dissolved in degassed anhydrous THF (200 mL) and cooled at −60 °C under argon. ^{t}BuLi (1.7 mol L^{-1} in pentane, 19.7 mL, 33.4 mmol) was added dropwise to this solution. The temperature should not get over −55 °C. The solution, initially colorless, turned yellow. After the reaction mixture has been stirred for 1 h at −60 °C, the temperature was allowed to rise to room temperature for a few minutes and brought down to 7 °C. This solution was then added to a degassed suspension of 1,10-phenanthroline (2.02 g, 11.2 mmol) in anhydrous THF (200 mL) kept between 5 and 7 °C. After stirring 4 h at 7 °C, the red solution was brought down to 0 °C and hydrolyzed with 1 mL of water. The reaction mixture was concentrated and extracted 3 times with CH_2Cl_2. The combined organic layers were thereafter rearomatized with MnO_2 under strong magnetic stirring, dried over $MgSO_4$, and filtered off on a sintered glass. The filtrate was evaporated to dryness. The crude product was purified by column chromatography (SiO_2, CH_2Cl_2) to give a brown oil in 86% yield (4.14 g, 9.6 mmol). NMR ^{1}H ($CDCl_3$, 200 MHz): 9.25 (dd, ^3J = 4.4 Hz, ^4J = 1.7 Hz, 1H: H_9), 8.29−8.23 (m, 4H: $H_{o,4,7}$), 8.06 (d, ^3J = 8.6 Hz, 1H: H_3), 7.81 (d, ^3J = 8.6 Hz, 1H: H_5), 7.75 (d, ^3J = 8.6 Hz, 1H: H_6), 7.64 (dd, ^3J = 8.1 Hz, ^3J = 4.4 Hz, 1H: H_8), 7.05 (d, ^3J = 8.6 Hz, 2H: H_m), 1.4−1.2 (m, 3H: H_c), 1.16 (d, ^3J = 6.4 Hz, 18H: H_d). MS (FAB-MS): found m/z = 429.2 $[M + H]^+$, calcd 429.65.

Compound 3. 1-(6-Bromohexyl)-2-(2-tetrahydro-2*H*-pyranyl) ether (1.64 g, 9.5 mmol) and *p*-bromophenol (2.47 g, 9.3 mmol) were dissolved in DMF (100 mL) under argon. Potassium carbonate (6.57 g, 47.5 mmol) was added, and the solution was heated at 60 °C for 18 h. DMF was then removed, and the residue was taken up into H_2O/CH_2Cl_2. Extraction with CH_2Cl_2 and drying over Na_2SO_4 left, after the solvent was removed, a crude which was purified by chromatography (SiO_2, eluent: CH_2Cl_2) to afford **3** (881 mg, 2.47 mmol) in 26% yield. NMR ^{1}H ($CDCl_3$, 200 MHz): 7.31 (d, ^3J = 8.9 Hz, 2H: H_m), 6.62 (d, ^3J = 8.9 Hz, 2H: H_o), 4.53 (m, ^3J = 2.9 Hz, 1H: H_α), 3.87 (t, ^3J = 6.4 Hz, 2H: H_1), 3.67 (t, ^3J = 6.2 Hz, 2H: H_6), 3.60 (m, 2H: H_ϵ), 2.06−1.21 (m, 14H: $H_{2,3,4,5,\delta,\beta,\chi}$).

Difunctionalized Phenanthroline 4. Compound **3** (2.14 g, 6.01 mmol) in degassed anhydrous THF (80 mL) was cooled at −60 °C under argon. ^{t}BuLi (1.7 mol L^{-1} in pentane, 7.5 mL, 12.0 mmol) was added dropwise to this solution. The solution, initially colorless, turned yellow. After the reaction mixture had been stirred for 3 h at −60 °C, the temperature was allowed to rise to room temperature for few minutes and brought down to −5 °C. This solution was then added to a degassed solution of **2** (1.7 g, 3.97 mmol) in anhydrous THF (80 mL), at room temperature. After stirring 15 h, the red solution was hydrolyzed with 1.5 mL of water and then turned orange. The reaction mixture was concentrated and extracted 3 times with CH_2Cl_2. The combined organic layers were rearomatized with MnO_2 under strong magnetic stirring, dried over $MgSO_4$, and filtered off on a sintered glass. The crude material was purified by column chromatography (SiO_2, CH_2Cl_2/0.1% MeOH) to give a brown oil in 86% yield (2.4 g, 3.41 mmol). NMR ^{1}H ($CDCl_3$, 200 MHz): 8.40 (m, 4H: $H_{o,o'}$), 8.26 (d, ^3J = 8.3 Hz, 2H: $H_{4,7}$), 8.08 (d, ^3J = 8.3 Hz, 2H: $H_{3,8}$), 7.74 (s, 2H: $H_{5,6}$), 7.10 (m, 4H: $H_{m,m'}$), 4.60 (m, 1H: H_α), 4.09 (t, ^3J = 6.4 Hz, 2H: $H_{1'}$), 3.95−3.38 (m, 4H: $H_{6',\epsilon}$), 1.92−1.20 (m, 17H: $H_{2',3',4',5',\beta,\chi,\delta,c}$), 1.15 (d, ^3J = 6.4 Hz 18H: H_d). MS (FAB-MS): found m/z = 705.4 $[M]^+$, calcd 705.03.

Compound 5. ^{n}Bu$_4$NF·3H$_2$O (0,37 g, 1.17 mmol) in 20 mL THF was added to a solution of **4** (0.676 g, 0.96 mmol) in THF (80 mL). The solution turned to orange and was stirred for 1.5 h. The THF was removed and the residue taken up into CH_2Cl_2. The organic layer was thoroughly washed with a buffer solution (pH 7), and then with pure water. After drying over Na_2SO_4 and removing of the solvent, an orange powder was recovered whose purity was good enough (>95% by NMR) to be used without purification. NMR ^{1}H ($CDCl_3$, 200 MHz): 8.37 (d, ^3J = 8.8 Hz, 2H: H_o), 8.25 (m, 4H: $H_{4,7,o'}$), 8.03 (d, ^3J = 8.8 Hz, 2H: H_3), 7.73 (s, 2H, $H_{5,6}$), 7.07 (d, ^3J = 8.8 Hz, 2H: H_m), 7.96 (d, ^3J = 8.6 Hz, 2H: $H_{m'}$), 4.62 (m, 1H: H_α), 4.05 (t, ^3J = 6.4 Hz, 2H: $H_{1'}$), 3.95−3.38 (m, 4H: $H_{6',\epsilon}$), 1.86−1.42 (m, 14H: $H_{2',3',4',5',\beta,\chi,\delta}$). MS (FAB-MS): found m/z = 549.2 $[M + H]^+$, calcd 549.69.

Monostoppered Thread 7. A mixture of **6** (1.93 g, 2.59 mmol) and **5** (1.23 g, 2.25 mmol) in 250 mL of degassed DMF was introduced under argon to a 1 L round-bottom flask containing Cs_2CO_3 (3.9 g, 1.19 mmol) in suspension in 180 mL of degassed DMF. The vessel was heated at 60 °C for 18 h. The solvent was removed and the residue taken up into CH_2Cl_2/H_2O. The organic layers were combined and dried over Na_2SO_4, and after the solvent was removed, the resulting brown solid was chromatographed (SiO_2, eluent CH_2Cl_2/1% MeOH) to give pure **7** in 82% yield. NMR ^{1}H ($CDCl_3$, 200 MHz): 8.36 (m, 4H: $H_{o,o'}$), 8.30 (m, 2H: $H_{4,7}$), 8.10 (m, 2H: $H_{3,8}$), 7.78 (s, 2H: $H_{5,6}$), 7.29−7.09 (m, 18H: $H_{m,m',a,b,d}$), 6.81 (d, ^3J = 9.1 Hz, 2H: H_c), 4.56 (m, 1H: $H_{\alpha'}$), 4.27 (m, 2H:

(22) Liptak, V. P.; Wulff, W. D. *Tetrahedron* **2000**, *56*, 10229−10248.
(23) Gibson, H. W.; Lee, S.-H.; Engen, P. T.; Lecavalier, P.; Sze, J.; Shen, Y. X.; Bheda, M. *J. Org. Chem.* **1993**, *58*, 3748−3756.
(24) Dietrich-Buchecker, C.; Sauvage, J.-P. *Tetrahedron* **1990**, *46*, 503−512.
(25) Livoreil, A.; Sauvage, J.-P.; Armaroli, N.; Balzani, V.; Flamigni, L.; Venturi, B. *J. Am. Chem. Soc.* **1997**, *119*, 12114−12124.

$H_{1'}$), 4.18−3.33 (m, 12H: $H_{6',\epsilon',\alpha,\beta,\chi,\delta}$), 1.80−1.50 (m, 14H: $H_{2',3',4',5',\beta',\chi',\delta'}$), 1.26 (s, 27H, $-CH_3$). MS (FAB-MS): found *m*/*z* = 1123.6 $[M]^+$, calcd 1123.6.

Alcohol 8. Compound **7** (2.06 g, 1.83 mmol) was dissolved in $CHCl_3$ (20 mL) in a 100 mL round-bottom flask equipped with a condenser. EtOH (40 mL) was added, and the solution was heated at 80 °C. Concentrated HCl (1 drop) was then added, and the mixture was refluxed for 3 h. The solvents were removed in a vacuum, and the residue was taken up into H_2O/CH_2Cl_2. The organic layer was washed with an aqueous saturated solution of K_2CO_3 and then with pure H_2O. Drying over Na_2SO_4 left, after the solvent was removed, a white powder whose purity was good enough (>95% by NMR) to be used without purification. NMR ^{1}H ($CDCl_3$, 200 MHz): 8.38 (m, 4H: $H_{o,o'}$), 8.27 (m, 2H: $H_{4,7}$), 8.08 (m, 2H: $H_{3,8}$), 7.75 (s, 2H: $H_{5,6}$); 7.26−7.07 (m, 18H: $H_{m,m',a,b,d}$), 6.79 (d, ^3J = 8.8 Hz 2H: H_c), 4.25 (m, 2H: $H_{1'}$), 3.61−3.15 (m, 10H: $H_{6',\alpha,\beta,\chi,\delta}$), 1.84−1.50 (m, 8H: $H_{2',3',4',5'}$), 1.27 (s, 27H: $-CH_3$). MS (FAB-MS): found *m*/*z* = 1039.5 $[M]^+$, calcd 1039.4.

Mesylate 9. Compound **8** (1.24 g, 1.195 mmol) and triethylamine (1.99 mL, 14.3 mmol) were dissolved in dry CH_2Cl_2 (35 mL) under argon. The mixture was then cooled to −5 °C. Mesyl chloride (0.55 mL, 7.17 mmol) in CH_2Cl_2 (20 mL) was added over 30 min, and the reaction mixture was then stirred for 5 h at −5 °C and 14 h at room temperature. The solution was extracted with H_2O/CH_2Cl_2 and dried over Na_2SO_4. The solvents were removed, and the brown crude product was chromatographed (SiO_2, eluent: CH_2Cl_2/0.2% MeOH) to afford **9** (1.23 g, 1.10 mmol) in 92% yield. NMR ^{1}H ($CDCl_3$, 200 MHz): 8.32 (m, 4H: $H_{o,o'}$), 8.21 (m, 2H: $H_{4,7}$), 8.03 (m, 2H: $H_{3,8}$), 7.69 (s, 2H: $H_{5,6}$), 7.20−7.01 (m, 18H: $H_{m,m',a,b,d}$), 6.72 (d, ^3J = 8.8 Hz, 2H: H_c), 4.18−3.81 (m, 12H: $H_{1',6',\alpha,\beta,\chi,\delta}$), 2.89 (s, 3H, -mesyl), 2.00−1.50 (m, 8H: $H_{2',3',4',5'}$), 1.32 (s, 27H: $-CH_3$). MS (FAB-MS): found *m*/*z* = 1117.5 $[M]^+$, calcd 1117.51.

Thioacetate 10. A solution containing a mixture of **9** (0.189 g, 0.169 mmol) and potassium thioacetate (25.5 mg, 0.223 mmol) dissolved in DMF (60 mL) was heated to 60 °C for 15 h. The DMF was removed and the residue taken up into CH_2Cl_2/H_2O. The organic layers were combined and dried over Na_2SO_4, and after the solvent was removed, the resulting brown solid was chromatographed (SiO_2, eluent CH_2Cl_2/0.2% MeOH) to give pure **10** in 80% yield. NMR ^{1}H ($CDCl_3$, 200 MHz): 8.41 (m, 4H: $H_{o,o'}$), 8.29 (m, 2H: $H_{4,7}$),8.10 (m, 2H: $H_{3,8}$), 7.78 (s, 2H: $H_{5,6}$), 7.27−7.08 (m, 18H: $H_{m,m',a,b,d}$), 6.81 (d, ^3J = 8.8 Hz, 2H: H_c), 4.30−3.90 (m, 10H: $H_{1',\alpha,\beta,\chi,\delta}$), 2.89 (t, ^3J = 7.1 Hz, 2H: $H_{6'}$), 2.30 (s, 3H, $-CH_3$ (thioester)), 2.00−1.50 (m, 8H: $H_{2',3',4',5'}$), 1.29 (s, 27H: $-CH_3$). MS (FAB-MS): found *m*/*z* = 1097.5 $[M]^+$, calcd 1097.52.

Semi-Rotaxane Cu(**10**.**11**)BF_4. By the cannula transfer technique, 23.9 mg (0.075 mmol) of $Cu(CH_3CN)_4BF_4$ in degassed acetonitrile (8 mL) was added under argon and at room temperature to a stirred degassed solution of **11** (33.7 mg, 0.059 mmol) in CH_2Cl_2 (10 mL). A deep orange coloration appeared instantly. After 15 min at room temperature, a solution of **10** (64.7 mg, 0.058 mmol) in CH_2Cl_2 (15 mL) was added to the solution which immediately turned dark red. After the solution was stirred for 2 h under argon at room temperature, the solvents were removed under high vacuum. A dark red powder of crude Cu(**10**.**11**)BF_4 was obtained quasi-quantitatively (NMR control) (106 mg, 0.058 mmol). Due to its instability on alumina and on silica gel, Cu(**10**.**11**)BF_4 was not further purified and was submitted to the next step without delay. NMR ^{1}H (CD_2Cl_2, 200 MHz): 8.61 (d, ^3J = 7.8 Hz, 2H: H_4), 8.59 (d, ^3J = 7.8 Hz, 2H: H_7), 8.42 (d, ^3J = 8.3 Hz, 2H: $H_{4''}$), 8.21 (s, 2H: $H_{5,6}$), 7.98 (s, 2H: $H_{5''}$), 7.99 (m, 2H: $H_{3,8}$), 7.97 (d, ^3J = 8.3 Hz, 2H: $H_{3''}$), 7.47 (d, ^3J = 8.7 Hz, 2H: H_o), 7.43 (d, ^3J = 8.7 Hz, 2H: $H_{o'}$), 7.29−7.09 (m, 18H: $H_{o'',a,d,b}$), 6.82 (d, ^3J = 8.8 Hz, 2H: H_c), 6.05 (m, 4H: $H_{m,m'}$), 5.96 (d, 4H, $H_{m''}$, ^3J = 8.6 Hz), 4.15 (m, 2H: H_δ), 3.91−3.45 (m, 28H: $H_{\gamma,\alpha',\beta,\beta',\alpha,\gamma',\delta',1',\epsilon'}$), 2.87 (t, ^3J = 7.3 Hz, 2H: $H_{6'}$), 2.29 (s, 3H: $-CH_3$ (thioester)), 1.51−0.80 (m, 8H: $H_{2',3',4',5'}$), 1.26 (s, 27H: $-CH_3$). MS (FAB-MS): found *m*/*z* = 1726.6 [Cu(**10**.**11**)]$^+$, calcd 1725.70; 1159.4 [Cu(**10**)]$^+$, calcd 1761.06; 629.1 [Cu(**11**)]$^+$, calcd 628.18.

Copper(I) Double Rotaxane $Cu_2$12$(BF_4)_2$. To a solution of Cu(**10**.**11**)BF_4 (27 mg, 0.015 mmol) in THF (10 mL) was added 15 mL of MeOH and a few grids of DMAP. HBF_4 (34%, 1 drop) was then added, and the mixture was heated to 60 °C for 5 days. The solvent was removed and the residue taken up into CH_2Cl_2/H_2O. The organic layers were combined and dried over Na_2SO_4, and after the solvent was removed, the resulting dark red crude material was chromatographed (Al_2O_3, eluent CH_2Cl_2/MeOH 2%) to give Cu_2**12**$(BF_4)_2$ in 53% yield.

NMR ^{1}H (CD_2Cl_2, 200 MHz): 8.61 (d, ^3J = 8.6 Hz, 4H: H_4), 8.60 (d, ^3J = 8.6 Hz, 4H: H_7), 8.44 (d, ^3J = 8.3 Hz, 4H: $H_{4''}$), 8.22 (s, 4H: $H_{5,6}$), 8.00 (s, 4H: $H_{5''}$), 7.86 (m, 4H: $H_{3,8}$), 7.81 (d, ^3J = 8.3 Hz 4H: $H_{3''}$), 7.49 (d, ^3J = 8.3 Hz, 4H: H_o), 7.44 (d, ^3J = 8.5 Hz 4H: $H_{o'}$), 7.27−7.07 (m, 36H: $H_{o'',a,d,b}$), 6.83 (d, ^3J = 8.5 Hz, 4H: H_c), 6.06 (m, 8H: $H_{m,m'}$), 5.97 (d, ^3J = 8.6 Hz, 8H: $H_{m''}$), 4.18 (m, 4H: H_δ), 3.90−3.42 (m, 56H: $H_{\gamma,\alpha',\beta,\beta',\alpha,\gamma',\delta',1',\epsilon'}$), 2.74 (t, ^3J = 7.2 Hz, 4H: $H_{6'}$), 1.60−0.83 (m, 16H: $H_{2',3',4',5'}$), 1.25 (s, 54H: $-CH_3$). MS (FAB-MS): found *m*/*z* = 3455.9 $([M - BF_4]^+$, calcd. 3456.0); *m*/*z* = 1684.0 $([M - 2BF_4]^{2+}$, calcd. 1684.4).

Thiol 13. Compound **10** (117.3 mg, 0.11 mmol) was dissolved in THF (15 mL) in a 50 mL round-bottom flask. Methanol (15 mL) and HCl 37% (3 mL) were added, and the mixture was stirred under argon at 60 °C for 6 days. The reaction was monitored by ^{1}H NMR. The mixture was brought to room temperature, and 20 mL of a buffer solution at pH 7 was then added. The solvents were removed, and the residue was taken up in CH_2Cl_2/H_2O. Extraction with CH_2Cl_2 and drying over Na_2SO_4 left, after the solvent was removed, a yellow solid whose purity was >95% (by NMR) and which was immediately used to do the threading step (see following paragraph). NMR ^{1}H (CD_2Cl_2, 300 MHz): 8.41 (m, 4H: $H_{o,o'}$), 8.30 (m, 2H: $H_{4,7}$), 8.10 (m, 2H: $H_{3,8}$), 7.79 (s, 2H: $H_{5,6}$), 7.28−7.14 (m, 18H: $H_{m,m',a,b,d}$), 6.81 (d, ^3J = 8.8 Hz, 2H: H_c), 4.26 (t, ^3J = 4.7 Hz, 2H: H_δ), 4.17−4.07 (m, 4H: $H_{\beta,\gamma}$), 3.98−3.91 (m, 4H: $H_{\alpha,1'}$), 2.55 (q, ^3J = 7.6 Hz, 2H: $H_{6'}$), 1.86 (m, 2H: $H_{5'}$), 1.72−1.50 (m, 6H: $H_{2',3',4'}$), 1.42 (t, ^3J = 7.8 Hz, 1H: −SH), 1.30 (s, 27H: $-CH_3$).

Threaded Copper(I) Complex. Cu(13.14)BF_4. By the cannula transfer technique, 25.3 mg (0.008 mmol) of $Cu(CH_3CN)_4BF_4$ in degassed acetonitrile (8 mL) was added under argon and at room temperature to a stirred degassed solution of **14** (49.5 mg, 0.008 mmol) in CH_2Cl_2 (10 mL). A deep orange coloration appeared instantly. After 15 min at room temperature, a solution of **13** (77 mg, 0.008 mmol) in CH_2Cl_2 (15 mL) was added to the solution which immediately turned dark red. After the solution was stirred for 2 h under argon at room temperature, the solvents were removed under high vacuum. A dark red powder of crude Cu(**13**.**14**)PF_6 was obtained quantitatively (the purity was controlled by ^{1}H NMR) and immediately submitted to the next reaction (see the following text).

Copper(I) Double Rotaxane. $Cu_2$15$(PF_6)_2$. A solution of Cu(**13**.**14**)BF_4 (140 mg, 0.007 mmol) in CH_2Cl_2 (10 mL) was stirred in air for 2 h. After removing the solvent and exchanging the counterions BF_4^- by PF_6^-, the resulting dark red solid was purified by several flash column chromatographies (Al_2O_3 ; eluent CH_2Cl_2/MeOH 0−2%) to give a dark red powder (68 mg, 50%). NMR

^{1}H (CD_2Cl_2, 400 MHz): 8.75 (d, ^3J = 8.4 Hz, 4H: H_{t3}), 8.63 (d, ^3J = 1.8 Hz, 4H: H_{t6}), 8.43−8.38 (m, 12H: $H_{4'',4,7,t3'}$), 8.05 (t, ^3J = 7.6 Hz, 2H: $H_{t4'}$), 7.94 (s, 4H: $H_{5''}$), 7.78 (d, ^3J = 8.3 Hz, 4H: $H_{3''}$), 7.72−7.63 (m, 12H: $H_{t4,3,8,5,6}$), 7.33 (d, ^3J = 8.7 Hz, 8H: $H_{o''}$), 7.30−7.12 (m, 36H: $H_{o',o,a,b,d}$), 6.83 (d, ^3J = 8.8 Hz, 4H: H_c), 6.03−5.95 (m, 16H: $H_{m',m,m''}$), 4.16 (m, 4H: H_δ), 3.88 (m, 4H: H_γ), 3.77 (m, 4H: H_β), 3.70 (m, 4H: H_α), 3.53 (t, ^3J = 6.7 Hz, 4H, $H_{1'}$), 3.21 (t, ^3J = 6.8 Hz, 8H: $H_{\gamma'}$), 2.91 (m, 8H: $H_{\alpha'}$), 2.75 (t, ^3J = 7.2 Hz, 4H: $H_{6'}$), 2.11 (m, 8H: $H_{\beta'}$), 1.75 (m, 4H: $H_{5'}$), 1.62 (m, 4H: $H_{2'}$), 1.55−1.30 (m, 8H: $H_{4',3'}$), 1.27 (s, 54H: $-CH_3$). MS (FAB-MS): found m/z = 3738.1 ($[M - PF_6]^+$, calcd 3736.7), m/z = 1795.5 ($[M - 2PF_6]^{2+}$, calcd 1795.8).

Acknowledgment. We are grateful to the French Ministry of Education for a fellowship to C.H. and the CNRS and the European Community for financial support.

Supporting Information Available: Cyclic voltammogram of copper-complexed [3]rotaxane Cu_2**12**$^{2+}$ in solution (Figure S1), cyclic voltammogram of copper(I)-complexed [3]rotaxane Cu_2**15**$^{2+}$ (Figure S2a), and the cyclic voltammogram of copper(II)-complexed [3]rotaxane Cu_2**15**$^{4+}$ obtained by anodic oxidation of Cu_2**15**$^{2+}$ (Figure S2b). This material is available free of charge via the Internet at http://pubs.acs.org.

IC0347034